Source characterization for automotive applications using innovative techniques

Harvie, J.; de Klerk, D.

DOI
10.1007/978-3-030-47630-4_10

Publication date
2021

Document Version
Final published version

Published in
Dynamic Substructures

Citation (APA)
Harvie, J., & de Klerk, D. (2021). Source characterization for automotive applications using innovative techniques. In A. Linderholt, M. Allen, & W. D'Ambrogio (Eds.), *Dynamic Substructures: Proceedings of the 38th IMAC, A Conference and Exposition on Structural Dynamics, 2020* (Vol. 4, pp. 117-125). (Conference Proceedings of the Society for Experimental Mechanics Series). Springer. https://doi.org/10.1007/978-3-030-47630-4_10

Chapter 10
Source Characterization for Automotive Applications Using Innovative Techniques

J. Harvie and D. de Klerk

Abstract Transfer path analysis (TPA) and source characterization using the in-situ blocked force methodology is becoming increasingly common in the automotive world. While robust techniques exist for this type of characterization in general, there are certain conditions where the analysis is more straight-forward than others. In this work, several techniques are presented to help improve the characterization across different frequency ranges.

At the very low frequencies, where structures should behave rigidly, TPA results can be improved by filtering out any non-rigid body motion from a set of measured FRFs. In the mid-frequency range, testing can be simplified using a volume source to capture reciprocal FRFs and then predict sound levels at the driver's ear. In the mid- and high- frequency ranges, the addition of rotational FRFs can help improve TPA predictions. These techniques are demonstrated using recent test results on various components and vehicles in this paper.

Keywords Transfer path analysis · Automotive · Frequency response functions · Blocked forces

Nomenclature

u	Dynamic displacements/rotations
f	Applied forces/moments
g	Interface forces/moments
Y	Admittance FRF matrix
$\star^{AB}$	Pertaining to the assembled system
$\star^{A}$;$\star^{B}$	Pertaining to the active/passive component
$\star_1$	Source excitation DoF
$\star_2$	Interface DoF
$\star_3$	Receiver DoF
$\star_4$	Indicator DoF
DoF	Degree of freedom
IDM	Interface displacement mode
FRF	Frequency response function
NTF	Noise transfer function
SNR	Signal to noise ratio
TPA	Transfer path analysis
VP	Vvirtual point

J. Harvie (✉)
VIBES.technology, Delft, The Netherlands
e-mail: jharvie@vibestechnology.com

D. de Klerk
VIBES.technology, Delft, The Netherlands

Delft University of Technology, Faculty of Mechanical, Maritime and Material Engineering, Department of Precision and Microsystems Engineering, Section Engineering Dynamics, Delft, The Netherlands

Müller-BBM VibroAkustik Systeme B.V, Hattem, The Netherlands

A. Linderholt et al. (eds.), *Dynamic Substructures, Volume 4*, Conference Proceedings of the Society for Experimental Mechanics Series, https://doi.org/10.1007/978-3-030-47630-4_10

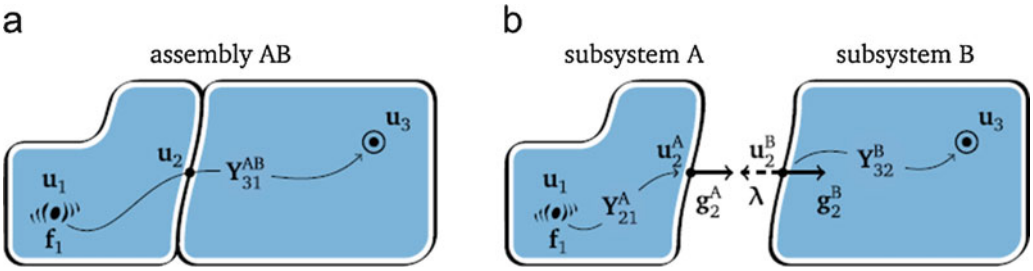

Fig. 10.1 The transfer path problem: (**a**) based on the admittance of assembly AB and (**b**) based on the admittances of subsystems A and B [1]

10.1 Background

Transfer path analysis is used to analyze the vibration transmission paths between an active source and a receiving structure. An in-depth overview of transfer path analysis techniques is provided in [1], and an overview is shown schematically in Fig. 10.1. Essentially, assembly AB consists of an active vibrating subsystem A and a passive receiving subsystem B. The system is excited by some force $\mathbf{f_1}$ that cannot easily be directly measured. It is desired to understand the response at the locations of interest $\mathbf{u_3}$ on the passive structure through an interface $\mathbf{u_2}$ due to this excitation.

The response at the locations of interest on the passive component can therefore be described using the system FRFs $\mathbf{Y_{31}^{AB}}$ with

$$\mathbf{u_3} = \mathbf{Y_{31}^{AB}}\mathbf{f_1} \tag{10.1}$$

While the internal excitation forces $\mathbf{f_1}$ are typically hard to measure and numerous, active sources are typically mounted with discrete points to their receivers. Hence finding an equivalent loadcase at the interface reduces the passive side loading to a manageable size / number. Such is the objective of component-based TPA, described next. Other families of TPA include classical TPA and transmissibility-based TPA, which are detailed in [1].

10.1.1 Component-Based TPA

Component-based TPA involves determining a set of equivalent forces that are a property of the source alone and can therefore be applied to an assembly AB with any receiving side B. When applied to system AB, the equivalent forces $\mathbf{f^{eq}}$ will yield the same responses $\mathbf{u_3}$ as the original source $\mathbf{f_1}$. Equivalent forces at the interface can be calculated using an in-situ approach [2, 3] with

$$\mathbf{f_2^{eq}} = \left(\mathbf{Y_{42}^{AB}}\right)^{+}\mathbf{u_4} \tag{10.2}$$

where $\mathbf{u_4}$ indicator sensors around the interface are used to improve the conditioning of the FRF matrix $\mathbf{Y_{42}^{AB}}$. This FRF matrix contains responses at the indicator sensors and inputs at the interface degrees of freedom (DoF). The equivalent force in Eq. 10.2 is often referred to as a blocked force in the literature, as the forces acquired will ideally be equal to the forces that would be measured if subsystem A was rigidly fixed or blocked at the interface. The equivalent forces can be validated by applying them to the assembly AB with

$$\mathbf{u_3} = \mathbf{Y_{32}^{AB}}\mathbf{f_2^{eq}} \tag{10.3}$$

and comparing the synthesized responses $\mathbf{u_3}$ to validation measurements. Equation 10.3 can also be used to predict responses of interest for new assemblies containing the active component A, as the equivalent forces are a property of only the source.

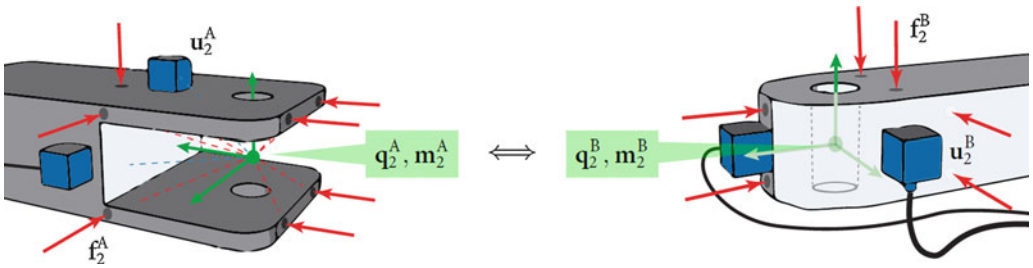

Fig. 10.2 Schematic showing the virtual point transformation [4]

10.1.2 Virtual Point Transformation

Additionally, to obtain the FRFs in Eqs. 10.2 and 10.3 with references exactly at the interfaces, the virtual point (VP) transformation can be used. With respect to TPA, the virtual point transformation can be used to provide a full 6-DoF description of the forces and moments acting exactly at the interface. The VP transformation is shown schematically in Fig. 10.2 and further detailed in [4]. Using this technique, forces are applied in a typical manner using an impact hammer or shaker, and a geometry-based transformation matrix is used to transform the FRF to have inputs exactly at the desired interface node(s), including both translations and rotations.

Essentially, this transformation can be written using interface displacement modes (IDMs) as

$$\mathbf{u} = \mathbf{R_u q} \quad \Rightarrow \quad \mathbf{q} = (\mathbf{R_u})^{+}\mathbf{u} \tag{10.4}$$

$$\mathbf{m} = \mathbf{R_f}^{\mathbf{T}}\mathbf{f} \quad \Rightarrow \quad \mathbf{f} = \left(\mathbf{R_f}^{\mathbf{T}}\right)^{+}\mathbf{m} \tag{10.5}$$

where the measured responses $\mathbf{u}$ are transformed to the $\mathbf{q}$ virtual point responses using the response IDM matrix $\mathbf{R_u}$, and similarly the measured forces $\mathbf{f}$ are transformed to the $\mathbf{m}$ virtual point forces and moments using the force IDM matrix $\mathbf{R_f}$. The IDM matrices are constructed to accurately characterize the problem at hand, often using six degrees of freedom (three translations and three rotations). The sensors and excitations are typically placed close to the virtual point such that rigid IDMs are used; however flexible IDMs can also be included.

The consistency functions detailed in [5] can be used to assess whether the chosen IDMs accurately represent the observed dynamics. The sensor consistency is essentially calculated by transforming the measured responses to the virtual point, projecting the virtual point responses back to the original coordinate system, and comparing the "filtered" responses with the original raw signals. This produces a frequency-dependent metric that is equal to 1 if all sensor responses are accurately described by the chosen IDMs. A similar calculation can be done for the impacts. The sensor and impact consistencies are typically assessed for the measurements made around each of the attachment points of an active source.

10.1.3 Techniques Presented Here

In-situ blocked force TPA using the virtual point transformation is becoming increasingly common in the automotive world. Under typical testing conditions where impact testing performs well, the TPA results are generally quite good. However there are certain conditions where the results can be improved using the techniques described below.

Rigidness Correction for Low Frequency TPA

At low frequencies (less than 20 or 50 Hz), it is often challenging to get enough consistent energy into large structures using a regular impact hammer. Data quality issues at the low frequencies are generally not uncommon when performing impact testing; for an overview of practical test considerations see [6]. These issues can be accepted in many applications where higher frequencies are the source of noise and vibration problems and the low frequency data quality is not paramount to the success of the analysis. However, for certain applications such as ride comfort, the lower frequencies can be of high interest.

For such cases, the consistency of the data at the low frequencies should be reviewed. At the very low frequencies, all sensors should move together, exhibiting rigid body motion. The sensor consistency can be used to assess the rigidness of

the data at these low frequencies. If the data are not consistent at the low frequencies, the virtual point transformation can be used to rigidify the FRFs. Using Eqs. 10.4 and 10.5, a set of FRFs can be transformed to a single 6-DoF virtual point near the center of an object, and then projected back to the original set of degrees of freedom.

However, this new set of FRFs will only be accurate in the frequency range where the test object behaves rigidly. Therefore, prior knowledge of the first flexible mode of the test object should be used to select a cutoff frequency where the rigidified FRFs can be cross-faded into the original set of FRFs. Additionally, the FRF matrix will now be very poorly conditioned at the low frequencies where the data has been rigidified, containing only six substantial singular values to represent whatever FRF size has been measured. To use the new FRF matrix for in-situ TPA, or any activities involving a matrix inverse, only the first six singular values should be included in a truncated inverse. The new hybrid set of FRFs should produce more accurate TPA results at the lower frequencies while leaving the higher frequencies unaffected.

Reciprocal FRFs for Mid-Frequency TPA Predictions

As noted in Eq. 10.3, component-based TPA can be used to predict responses of interest (accelerations or sound pressure levels) using equivalent forces and the FRFs of the assembled system. The FRFs $\mathbf{Y}_{32}^{\mathbf{AB}}$ contain the responses at the locations of interest relative to the interface degrees of freedom. This FRF matrix is usually obtained by making several impacts around each interface and measuring the responses of interest. However, these FRFs can be obtained in an alternative way due to the property of reciprocity. Due to reciprocity, we can instead measure $\mathbf{Y}_{32}^{\mathbf{AB}}$, with inputs at the locations where responses are desired, and outputs at the interface degrees of freedom. A review of reciprocity in this context is provided in [7, 8]. Practically, this means installing sensors around the interfaces, and then exciting the structure at the locations of interest using either an impact hammer for structural interests or a volume source for acoustic interests. The actual testing time will be greatly reduced for a test of this form. These FRFs can then be used in TPA predictions across whatever frequency range has good coherence, which is typically best in the mid-frequency range.

Rotational FRFs for Mid- to High-Frequency TPA

In general, it is easier to measure translational forces than rotational moments for both classical and component-based TPA. While 6-DoF force gauges exist that can be used to directly measure forces and moments, those force gauges can often be substantial in size, and therefore may not be able to measure the desired quantities exactly at the interfaces. With FRF-based TPA techniques, impact hammers are naturally only able to measure translational force inputs. Thus, TPA is often performed using only translational forces. TPA using only translational forces is likely accurate at low frequencies in most cases where the behavior of the components and systems is fairly rigid.

However, with the current trends in the automotive industry shifting toward electric vehicles and components, higher frequencies are becoming more and more relevant and troublesome. At the higher frequencies where the dynamics are more complex, translational forces alone are likely inadequate for source characterization. It will be shown that including rotational degrees of freedom in the virtual point transformation can improve the results at those higher frequencies.

The advantages of including rotations in source characterization have previously been discussed in [9] where the recommendation to include rotations in two upcoming ISO standards [10] [11] was introduced. Additionally, the use of an on-board validation sensor to validate the accuracy of the calculated blocked forces is also presented in [9] and will be used in this work.

10.2 Analysis

10.2.1 Rigidness Correction for Low Frequency TPA

An active component was recently tested on a rigid test bench to determine blocked forces using various methods. The structure was equipped with 32 tri-axial accelerometers (96 channels) during both FRF testing and operational measurements, in order to calculate in-situ blocked forces with Eq. 10.2.

The consistency of these sensors during FRF testing is shown in the left side of Fig. 10.3. As seen in the figure, the consistency is close to 100% from around 20 to 40 Hz. This means that all sensors are moving rigidly together in this frequency range. There are modes of the structure above 40 Hz (related to both the component and the test bench), so the consistency of all sensors is not expected to be high in that frequency range. However, at frequencies below 20 Hz, the structure should be moving rigidly and the sensor consistency should be higher than it is. It is believed that the poor consistency in this frequency range is primarily due to poor signal-to-noise ratio (SNR) on the very stiff test bench.

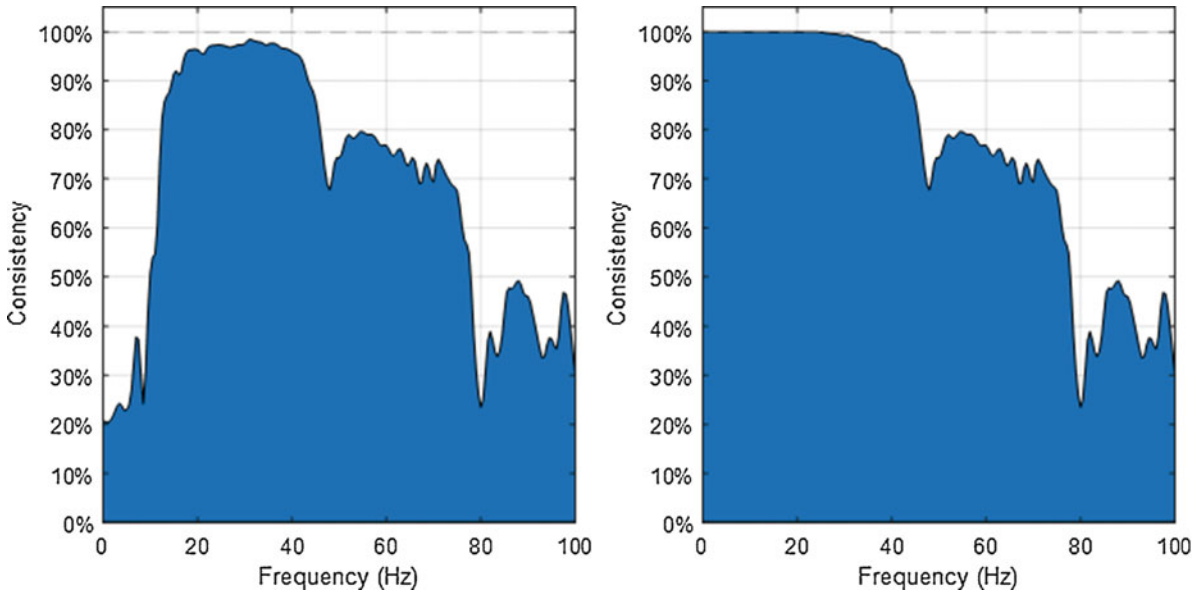

Fig. 10.3 Sensor consistency of (left) raw FRF data and (right) rigidified FRF data

The FRFs were then transformed to a single 6-DoF virtual point and projected back to the original degrees of freedom, as described above. This set of rigidized FRFs was merged with the original FRFs with a cutoff frequency centered at 25 Hz. The sensor consistency of the new set of FRFs is presented on the right side of Fig. 10.3. As expected, the "filtered" FRFs behave very rigidly and consistently at the low frequencies, while leaving the sensor consistency at higher frequencies unaffected.

An operational test with broadband content was then performed to do in-situ source characterization and TPA. Of the 32 sensors used in the test, 30 were used as indicators (u_4) and 2 were used as validation sensors (u_3). A total of 40 interface DoF were considered. The blocked forces were calculated using both the raw FRFs and the rigidified FRFs. These blocked forces were applied to the system using Eq. 10.3, and TPA results are compared to the measured response at one of the validation sensors in Fig. 10.4. As seen, both predictions match the measured response well at higher frequencies, but there is a discrepancy between the measured response and the raw FRF TPA at very low frequencies (below 10 Hz). By rigidifying the FRFs, the TPA results are greatly improved at those low frequencies.

10.2.2 Reciprocal FRFs for Mid-Frequency TPA Predictions

A separate test was recently done on a full vehicle for source characterization of the tire noise. Sensors were placed around each of the wheel hubs during FRF and operational tests, again for in-situ blocked force TPA. Impacts were made around each wheel hub and transformed to virtual points, and these virtual point FRFs were used to calculate blocked forces during a constant speed test with Eq. 10.2.

For this test series, the response of interest was the sound at the driver's ear. To calculate this response due to the blocked forces, two sets of FRFs were measured. First, the FRFs $\mathbf{Y}_{32}^{\mathbf{AB}}$ between a microphone at the driver's ear and the impacts at the wheel hubs were measured, as is usually done. Additionally, a low frequency volume source (LFS) was placed at the driver's ear position, and the accelerometers around the wheel hubs were used to measure $\mathbf{Y}_{23}^{\mathbf{AB}}$. A sample noise transfer function (NTF) from the volume source measurement is shown in Fig. 10.5 where the coherence looks reasonable up to approximately 500 Hz.

A few comparisons between the impact test and the volume source NTFs are shown in Fig. 10.6 and Fig. 10.7. Most of the NTFs compare quite well, with similar quality as in Fig. 10.6. Some of the comparisons are not quite as good, as in Fig. 10.7; the worse comparisons are generally for rotational DoF. There are a couple possible reasons for the discrepancies. There may be inaccuracies in the impact measurements that are more pronounced in the rotational DoF. There could also be inaccuracies in the accelerometer responses during the volume source measurement, as the discrepant region is near the region of low coherence in Fig. 10.5. The primary cause of the discrepancies was not further investigated.

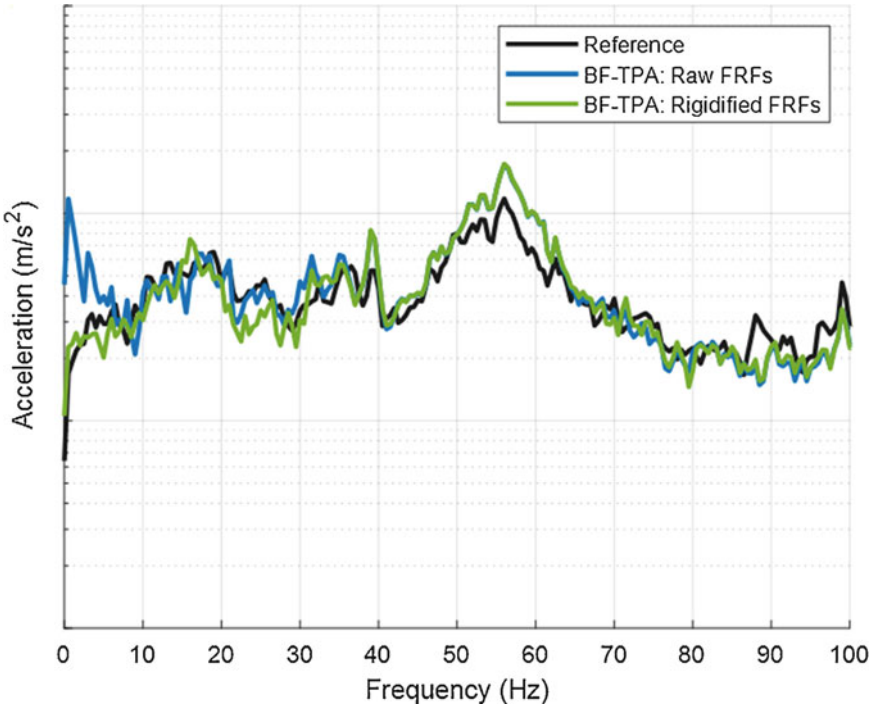

Fig. 10.4 Blocked force TPA validation using raw FRFs and rigidified FRFs

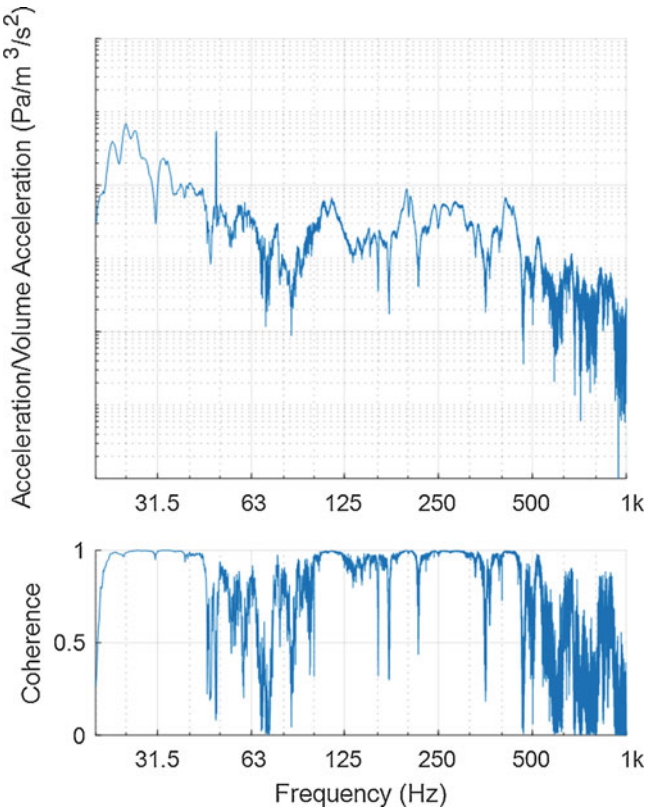

Fig. 10.5 Sample FRF data quality between the volume source and an accelerometer

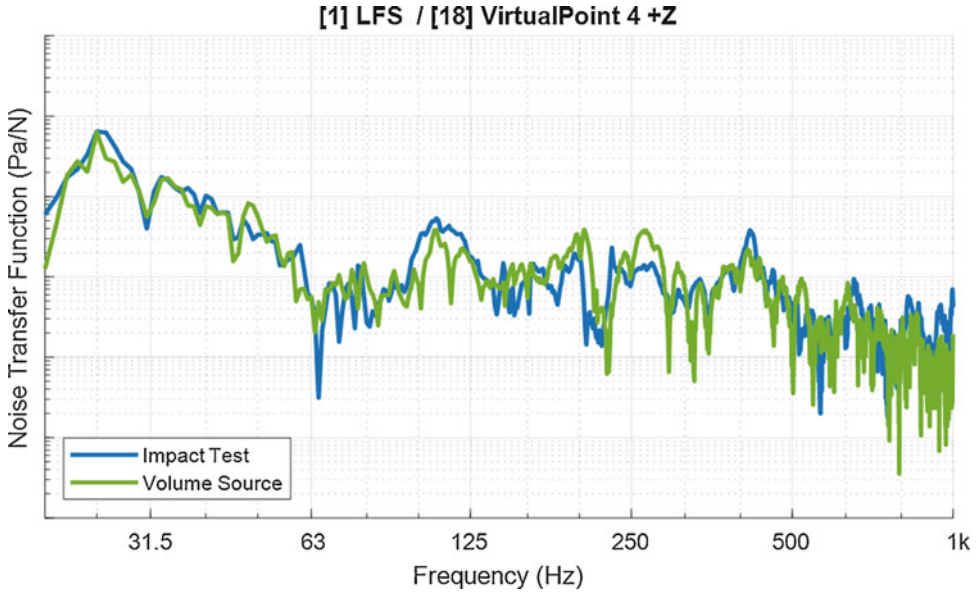

Fig. 10.6 Comparison between noise transfer functions using impact hammer and volume source, "best" comparison

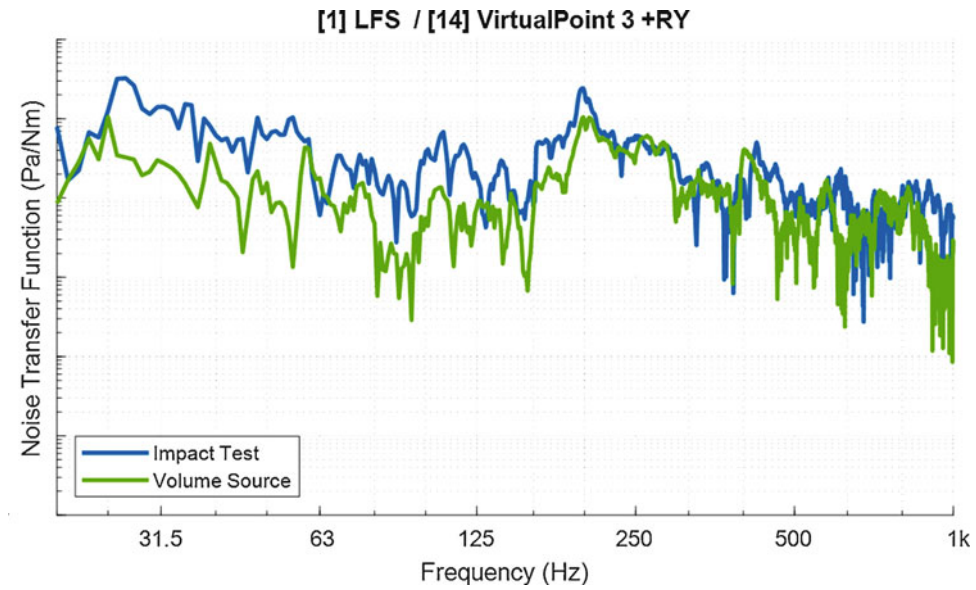

Fig. 10.7 Comparison between noise transfer functions using impact hammer and volume source, "worst" comparison

The calculated blocked forces were applied to both sets of NTFs to predict the sound at the driver's ear during a constant speed environment, with results shown in Fig. 10.8. Both predictions compare well with the actual sound measured during the operational test. In general, the reciprocal volume source predictions do not perform notably better or worse than the impact test predictions. This suggests that there may be some small errors in the initial blocked force calculation that are propagating through to the validation, regardless of the technique used. This confirms that the reciprocal measurement can be used for TPA predictions in place of the impact test measurement.

10.2.3 Rotational FRFs for Mid- to High-Frequency TPA

Finally, another series of tests was done on a different active component on a test bench to perform in-situ blocked force TPA. Tests were run using three tri-axial accelerometers as indicators around each of the three attachment points. Impacts were

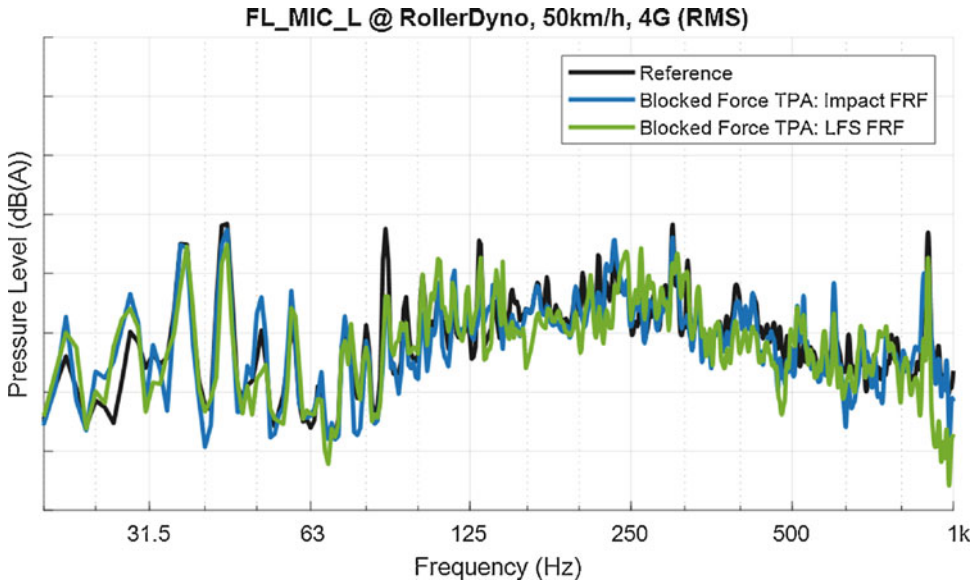

Fig. 10.8 Blocked force TPA in a constant speed roller dyno environment, comparison between impact and volume source FRFs

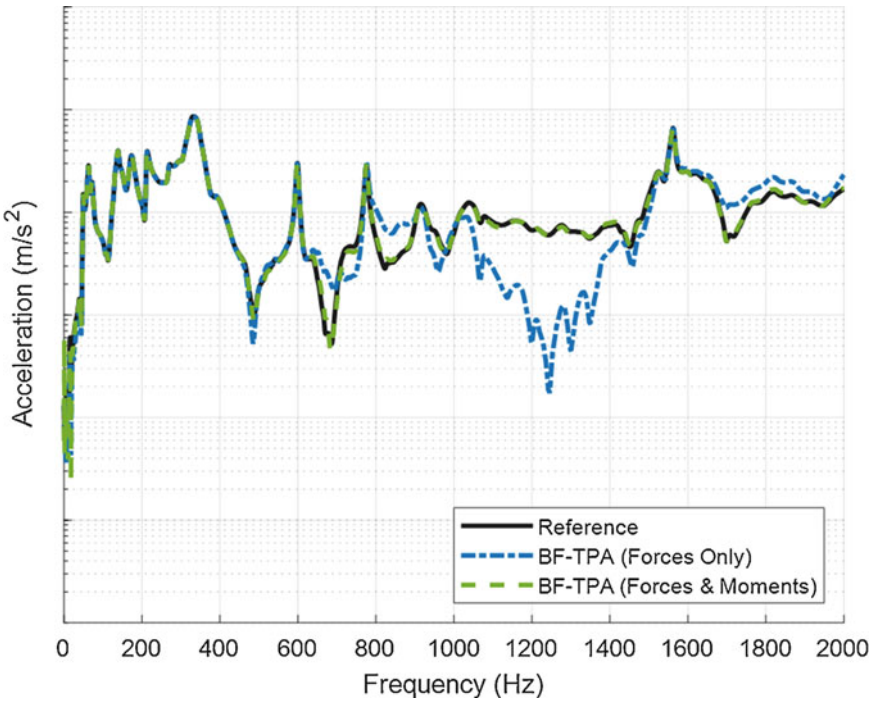

Fig. 10.9 Blocked force TPA validation using only forces as well as forces and moments

made around each attachment point and transformed to virtual points. Two sets of virtual points were considered. In the first set, each connection point was assumed to have three translational degrees of freedom. In the second set, each connection point was assumed to have three translational degrees of freedom as well as three rotational degrees of freedom.

Blocked forces were calculated for a controlled load case, using an impact on the component rather than an actual operational load condition to ensure reliable data. The response at a validation sensor was then calculated by applying the blocked forces to the system. In Fig. 10.9, the validation sensor responses are compared between the measured data and the TPA simulations with and without moments included. At lower frequencies, below ~600 Hz, both TPA simulations compare very well with the measured response. However at higher frequencies, the TPA using only translational forces deviates from the measured response, while the TPA using both translational forces and rotational moments continues to

match the measured response. This suggests that while translational measurements may produce accurate results at lower frequencies, it is important to include rotational effects as the analysis goes to mid- and high-frequency regions.

10.3 Conclusion

Transfer path analysis is used extensively in the automotive industry to characterize actively vibrating components. While current techniques provide reasonable analysis of the vibrations, there are several recent advances that can further improve the analyses. Here, it was shown how rigid body corrections can improve the very low frequency TPA results. It was also shown how using a volume source rather than impact testing can produce accurate TPA results in the mid-frequency range, and will also speed up test time. Finally, it was shown how including moments in a blocked force calculation can improve TPA results at higher frequencies over using just translational forces alone.

In the cases shown, it was very obvious which frequency ranges benefited from using the newer techniques. However, for different test structures and test setups, the appropriate frequency ranges to employ each technique will vary. It is important to think about the dynamics involved for any specific test case and use the appropriate methods to get an accurate characterization.

References

1. van der Seijs, M., de Klerk, D.: Rixen, D.J.: General framework for transfer path analysis: History, theory and classification of techniques. Mechanical Systems and Signal Processing, pp. 68–69, August 2015
2. Elliott, A.S., Moorhouse, A.T.: Characterisation of structure borne sound sources from measurement in-situ. J. Acoust. Soc. Am. **123**(5), 3176 (2008). https://doi.org/10.1121/1.2933261
3. Moorhouse, A.T., Elliott, A.S., Evans, T.A.: In situ measurement of the blocked force of structure-borne sound sources. J. Sound Vib. **325**(4–5), 679–685 (2009). https://doi.org/10.1016/j.jsv.2009.04.035
4. van der, Seijs, M., et al.: An improved methodology for the virtual point transformation of measured frequency response functions in dynamic substructuring. COMPDYN 2013, Kos Island, Greece, 12–14 June 2013
5. van der Seijs, M.: Experimental Dynamic Substructuring: Analysis and Design Strategies for Vehicle Development. PhD Thesis, Technische Universiteit Delft, June 2016
6. Allen, M.S., Rixen, D., van der Seijs, M., Tiso, P., Abrahamsson, T., Mayes, R.L.: Substructuring in Engineering Dynamics: Emerging Numerical and Experimental Techniques. CISM International Centre for Mechanical Sciences, Courses and Lectures, Volume 594, 2020, Section 4.5
7. Fahy, F.J.: Some applications of the reciprocity principle in experimental vibroacoustics. Acoust. Phys. **49**(2), 217–229 (2003)
8. ten Wolde, T.: Reciprocity measurements in acoustical and mechano-acoustical systems. Review of theory and applications. Acta Acust. United AC. **96**(1), 1–13 (2010)
9. van den Bosch, D., van der Seijs, M., de Klerk, D.: A Comparison of Two Source Characterisation Techniques Proposed for Standardisation. SAE Technical Paper 2019-01-1540, 05 June 2019
10. ISO/TC43/SC1: ISO/AWI 21955 Vehicles – Experimental Method for Transposition of Dynamic Forces Generated by an Active Component from a Test Bench to a Vehicle. International Organization for Standardization, Under Development, https://www.iso.org/standard/72288.html
11. ISO/TC43/SC1: ISO/DIS 20270 Acoustics – Characterization of Sources of Structure-Borne Sound and Vibration – Indirect Measurement of Blocked Forces. International Organization for Standardization, Under Development, https://www.iso.org/standard/67456.html